Exploratory study of the electrochemical properties of local cassava starch as a potential green and sustainable polymer binder for energy storage application

Article *in* MRS Advances · July 2023

DOI: 10.1557/s43580-023-00608-z

14 authors, including:

Latifatu Mohammed
CSIR - Council for Scientific and Industrial Research - Ghana
39 PUBLICATIONS **277** CITATIONS

SEE PROFILE

David Dodoo Arhin
University of Ghana
121 PUBLICATIONS **2,323** CITATIONS

SEE PROFILE

Rejart Adomah
CSIR - Institute of Industrial Research
5 PUBLICATIONS **7** CITATIONS

SEE PROFILE

Nafiu Zainudeen
University of Ghana
7 PUBLICATIONS **29** CITATIONS

SEE PROFILE

MRS Advances
https://doi.org/10.1557/s43580-023-00608-z

ORIGINAL PAPER

Exploratory study of the electrochemical properties of local cassava starch as a potential green and sustainable polymer binder for energy storage application

Latifatu Mohammed[1] · Wilson Tamakloe[2] · David Doodo‑Arhin[3] · Rejart Adomah[1] · Mohammed Nafiu Zainudeen[4,5] · Juliet Opoku[1] · Andrew Nyamful[5] · Benjamin Agyei‑Tuffour[3] · Alex Nyarko[6] · Mutala Mohammed[1] · Kofi Ampomah‑Benefo[1] · Trinity Ama Tagbor[1] · Francis Agyenim[1] · Jang Myoun Ko[7]

Received: 1 March 2023 / Accepted: 4 July 2023

Abstract

The need to develop an aqueous-based binder has dominated research publications for some time now. The application of this man-made aqueous-based binder in LIBs has the potential to reduce the environmental impact of LIB. In this preliminary study, local cassava starch is treated and prepared as a polymer binder for LIBs application. The binder is applied in lithium nickel manganese cobalt oxides electrodes as a cathode in LIBs. The electrodes displayed a discharge capacity of 142 mAh/g and 73 mAh/g for LiNMCO-442/Cassava starch and 139 and 28 mAh/g for LiNMCO-442/PVDF at 0.1 C-rate and 10 C-rate respectively. After 100 cycles, the LiNMCO-442 cells retained about 80.2 and 65.5% for the cells with cassava starch binder and PVDF binder, respectively, at room temperature. The fairly electrochemical performance of the local cassava starch makes it a potential alternative to the petroleum-based binder, PVDF.

Introduction

Climate change is the major challenge our world faces currently. The transition towards a climate-neutral globe needs fundamental changes in the approach to the generation and the use of energy. Lithium-ion batteries (LIB) could be true enablers if they could be manufactured from safer materials and provide superior performance, sustainability, and affordability. The quest to increase the number of electric vehicles on our roads as well as the necessity to store extra energy from renewable energy has brought all types of batteries into the limelight of many researchers and industrial players. To increase the energy density of LIB, different electrodes [1, 2], electrolytes [3, 4], separators [5, 6], and binder materials [7, 8] have been investigated. The LIB consists of electrodes (cathode and anode), the separator, and the electrolyte. Each of these components is very important in the battery performance. The electrode is made up of electro-active material coated on a current collector to facilitate the electrochemical reaction necessary to store charges. The binder is typically used in binding the electro-active materials and other additives to the current collector. Although the binder in the electrode is only a small fraction of the total weight of the LIB, they determine the slurry viscosity, porous morphology, electrical networking, and volume expansion of electro-active materials and the cycling performance of the battery cell [9]. The commonly used binder in the commercially available LIBs is a synthetic water-insoluble polymer, polyvinylidene difluoride (PVDF) [10]. It is normally dissolved in an environmentally toxic solvent such as N-methyl-2-pyrrolidone (NMP) [11]. The need to develop

---

✉ Latifatu Mohammed
Latifatu.mohammed@yahoo.com

[1] Institute of Industrial Research, Council for Scientific and Industrial Research, P. O. Box LG 587, Accra, Ghana

[2] Department of Material Science & Engineering, Korea University, Seoul 02841, Republic of Korea

[3] Department of Materials Science & Engineering, University of Ghana, Annie Jiaggie Road, Legon, Accra, Ghana

[4] Department of Fluid Science, CSIR-Institute for Scientific and Technological Information, P. O Box CT 2211, Accra, Ghana

[5] Department of Nuclear Engineering, Graduate School of Nuclear and Allied Sciences, University of Ghana, Accra, Ghana

[6] Avery Dennison, 171 Draketown Road, Pennsylvania, PA 17751, USA

[7] Department of Chemical and Biological Engineering, Hanbat National University, Daejeon 34158, Republic of Korea

an aqueous-based binder has dominated research publications for some time now [12, 13]. The application of bio-based polymer binders in LIBs has the potential to reduce the environmental and health impact of LIB with a drastic CO_2 reduction [14]. More significantly, PVDF is considered teratogenic and mutagenic, and NMP is also considered a teratogenic, hazardous, and irritating compound [15]. On the other hand, laboratory preparation of electrodes with aqueous-based binders has the advantage of easy evaporation of the dispersing medium (water) and shorter drying time compared to NMP based on the fact that the vapour pressure of water is 35 times greater than NMP [16]. Various efforts have been invested in finding alternative and sustainable binder material that works for the LIB cathode electrodes application. These binders include water-based polysaccharides-based binders such as polyacrylic acid, sodium carboxymethyl cellulose (CMC), sodium alginate, and starch [17, 18]. Although there has been widespread research on starch from different biomass materials as binders for LIB anode electrodes, little has been done with cassava starch as binders for LIB cathode application. In Zinc-air batteries, Masri et al. fabricated Zn-air batteries employing tapioca (cassava starch) as a binder for porous zinc anode. They found excellent adhesion of the zinc powder with the cassava binder [19]. In addition, Ismail et al. also investigated cassava starch as a conductive biodegradable material by coating a layer of cassava starch on a zinc anode. The electrodes showed an increase in conductivity by 30% and, therefore, improved the discharge capacity of the zinc anode [20]. In this preliminary study, we demonstrate the potential application of starch extracted from cassava as a polymeric binder in LIB cathode based on its electrochemical properties. Cassava is the staple food for lots of people in different parts of the globe, and it is widely cultivated in West Africa, the Caribbean, and Asia. Starch is the second most plentiful biomaterial in nature. It is eco-friendly because it is renewable and biodegradable, very cheap, and readily available [21]. The success of obtaining a sustainable, cheap, environmentally friendly, and commercially workable binder for LIB electrodes will contribute significantly to reducing the carbon footprint of LIB production and the promotion of sustainable development goals (SDG 7 and 13).

Experimental procedure

Characterization of dried cassava starch

The functional groups of atoms on the surface of the dried cassava starch were recorded on a Bomem MB100 (ABB Bomem, Canada) Fourier transforms infrared (FTIR) spectrometer. Spectra information was recorded within the 4000–600 cm^{-1} spectral range in transmission mode and analysed utilizing the GRAMS/AI™ Spectroscopy Software Suite. The thermal property of the cassava starch was conducted utilizing a Thermtest TGA-n 1000 thermal analyzer (Thermtest Instruments, USA) outfitted with the Infinity Pro Thermal Analysis software.

Preparation of cassava starch

The cassava starch was completely dried with a food hydrate at 60 °C for 6 h. 5 g of the dried starch was dispersed in 95 g of deionised water using a magnetic stirrer at 10 r.p.m for an hour at room temperature. The starch solution was mixed further for 3 h at 80 °C with a magnetic stirrer to obtain a clear gelatinised solution. For the control sample, 5 g of PVDF was dissolved in 95 g of NMP and stirred overnight with a magnetic stirrer at room temperature to obtain a homogenous mixture.

Fabrication of LiNMCO-442 electrode and characterization

Lithium nickel cobalt manganese oxide ($LiNi_{0.4}Mn0.4Co_{0.2}O_2$—LiNMCO-442) cathode was fabricated by casting a slurry consisting of 92% (LiNMCO-442, Ecopro, Korea) as active material, 3 wt% of the super-P as a conducting agent (Timical super PTM), 5 wt% of the gelatinised solution was used as an aqueous-based binder. The slurry was coated on an aluminium foil (15 µm, Korea) using a doctor blade's apparatus. The water was completely evaporated from the coated slurry at 120 °C for 2 h and then pressed with a roll pressing machine (Samyang 60, WV-60, Korea). For a control, 5 wt% polyvinylidene fluoride (PVDF, Mw = 350,000, Kreha, Japan) in N-methyl-2-pyrrolidone (NMP, Sigma Aldrich) was also prepared. The densities, thickness, and loading levels were controlled to about 1.9 g cm^{-3}, 49 µm, and 14 mg cm^{-2} correspondingly, for all the electrodes. The surface structure of the prepared electrodes was measured using a field-emission scanning electron microscope (FE-SEM, HITACHI SU5000, Japan).

Coin cell assembly and electrochemical property testing

The fabricated electrode sheets were cut into spherical discs with a diameter of 14 mm. The coin cell (2032) assembled in a glove box filled with argon was made up of LiNMCO-442 with the starch binder as the working electrode and lithium metal (Aldrich, 16 mm, 99.99%) as the reference and counter electrode. The electrolyte consists of 1.2 M LiPF6 dissolved in a mixture of ethylene carbonate and dimethyl carbonate (EC/DMC = 1:3) and the separator materials were polyethylene separator (celgard, 18 mm, 20 µm).

The cyclic voltammograms (CVs) of the LiNMCO-442 electrode with the cassava starch binder were obtained at a potential range of 2.5–4.4 V and a scan rate of 0.1 mV/s utilising Autolab (ECO CHEMIE PGSTAT 100). The charge/discharge performance was measured at ambient temperature in the potential range of 2.5–4.4 V, charging in a constant current/constant voltage mode at 0.1 C rate and discharging at a constant current mode at 0.1 C, 0.2 C, 0.5 C, 1.0 C, 2.0 C, 5.0 C, and 10.0 C rates employing PNE solution charge/discharge cycler. All the engineered cells were stored for 12 h before electrochemical testing. The resistance connected to the electrodes, separator, and electrolyte in the cells was examined using electrochemical impedance spectroscopy (EIS) in a frequency range of 0.01 Hz to 1 MHz at open-circuit potential (OCP).

Results and discussions

Thermal stability and FTIR characterization

The thermal properties of the dried cassava starch and PVDF samples are shown in Fig. 1a. The TGA curves for the cassava starch show mass losses in three stages: the first is due to dehydration. The second and third mass losses are attributed to the decomposition of organic matter (amylose and amylopectin) and the development of final residues (ash). The PVDF showed better thermal stability compared to the cassava starch. This may be a result of the restricted chain motion of the PVDF [22].

The FTIR spectra of the dried cassava starch and PVDF samples are shown in Fig. 1b. The absorption peaks at 610, 771, and 1002 cm^{-1} are the characteristic peaks of α-crystal shape. The absorption peaks at 592 and 852 cm^{-1} are the characteristic peaks of β-crystal shape in the PVDF [23]. The very strong band appearing at 1184 cm^{-1} is mainly composed of the CF_2 symmetric stretching mode. The band at 1219 cm^{-1} represents the coupling of the CF_2 asymmetric stretching mode and -C–C- symmetric stretching mode. The band at 856 cm^{-1} is assigned to the symmetric stretching vibration of the C–C bond with small contributions from the stretching of CF bond and deformation of the H–C–H angle. The CF_2-bending vibration is assigned to the strong band at 766 cm^{-1}.

The FTIR spectrum of the cassava starch shows the common signals of polysaccharides, with glucopyranose rings such as O–H bands at 3300 cm^{-1}, C–H stretching vibrations of aliphatic groups at 2926 cm^{-1}, adsorbed water signals at 1650 cm^{-1}, C–C and C–O stretching at 1160 cm^{-1}, and –COOH-bending vibration at 1005 cm^{-1} [24]. Furthermore, the absorbance peak at 1415 cm^{-1} implied the presence of C-H symmetrical scissoring of CH_2OH moiety. The presence of the –OH and –COOH functional groups in starch has been proven to interact with other functional groups on the surfaces of electro-active materials, to form bonds [25]

Surface morphology of LiNMCO-442 electrode with the cassava starch binder

The surface structure of the LiNMCO-442 electrodes with the cassava starch binder at different magnifications is depicted in Fig. 2. The LiNMCO-442 exhibited aggregates of secondary particles with an average size of about 10 µm and primary particles with an average size of around 50 nm. The micrograph of the fabricated electrode with the cassava starch and the PVDF binder revealed some bare LiNMCO-442 areas and conductive carbon/binder aggregation between the secondary particles of the LiNMCO-442. The images disclosed an equally dispersed composite of carbon additive/binder on the surface of the particles of LiNMCO-442, forming a strong linkage that infiltrates from the particles of the coated mass to the current collector, thereby providing better electronic conductivity. Furthermore, LiNMCO-442 with the cassava starch showed a more equally distributed and well-connected linkage with particle-to-particle contact compared to the LiNMCO-442 electrode with PVDF binder. This structure and interconnection facilitate good electronic and ionic conductivity, and this may be

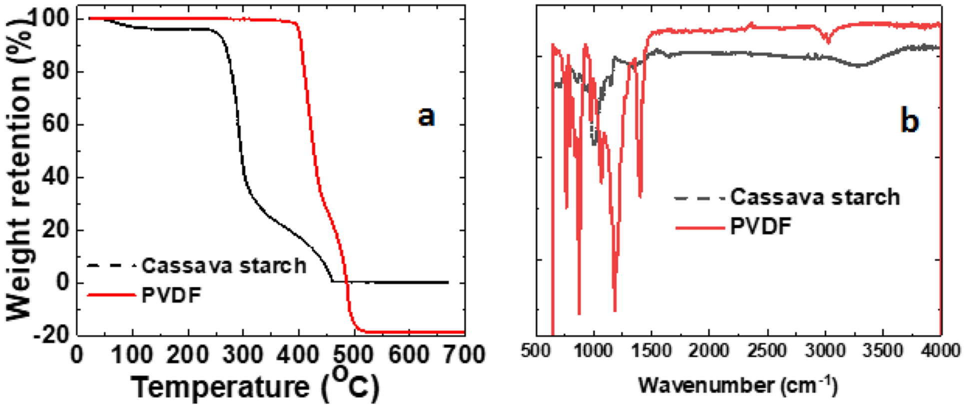

Fig. 1 **a** Thermogravimetric stability and **b** FTIR spectra of dried powder of PVDF and Cassava starch

responsible for the excellent rate capability at a higher c-rate (see Fig. 3e).

Electrochemical performance of LiNMCO-442 electrode with the cassava starch binder

The CV curves for the cells with cassava starch and the PVDF binder are displayed in Fig. 3. Both cells revealed an anodic peak of around 3.9 V and a cathodic peak of around 3.7 V, and this matches other publications [26]. These peaks can be ascribed to the redox activities of Ni^{2+}/Ni^{4+}, connected to the de-insertion and insertion of lithium ions into the crystal structure of LiNMCO-442. There is no peak corresponding to the reduction of Mn at 3.0 V; thus, it has an oxidation state of + 4. Referring to Table 1, the oxidation–reduction peak separation ΔE ($E_{oxidation}$-$E_{reduction}$) is in the order of LiNMCO-442/Cassava Starch < LiNMCO-442/PVDF. This suggests that the electrode with cassava starch polymer binder poses the least polarization and hence the excellent rate capability observed in Fig. 3 [27].

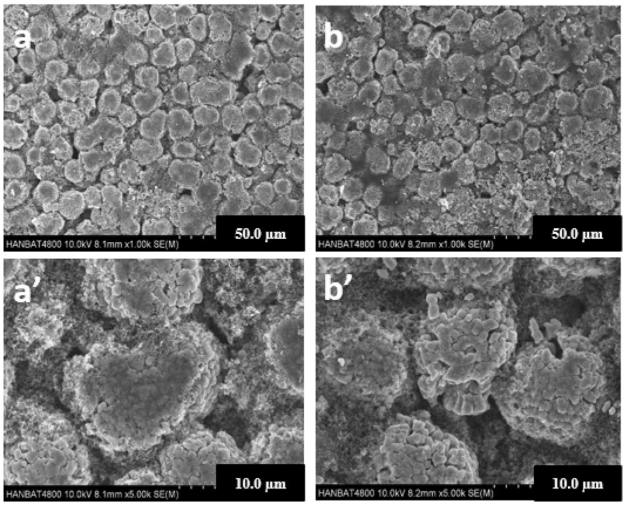

Fig. 2 FE-SEM micrographs at different magnifications for **a** (a') LiNMCO-442 with PVDF binder, *b* (b') LiNMCO-442 with cassava starch binder

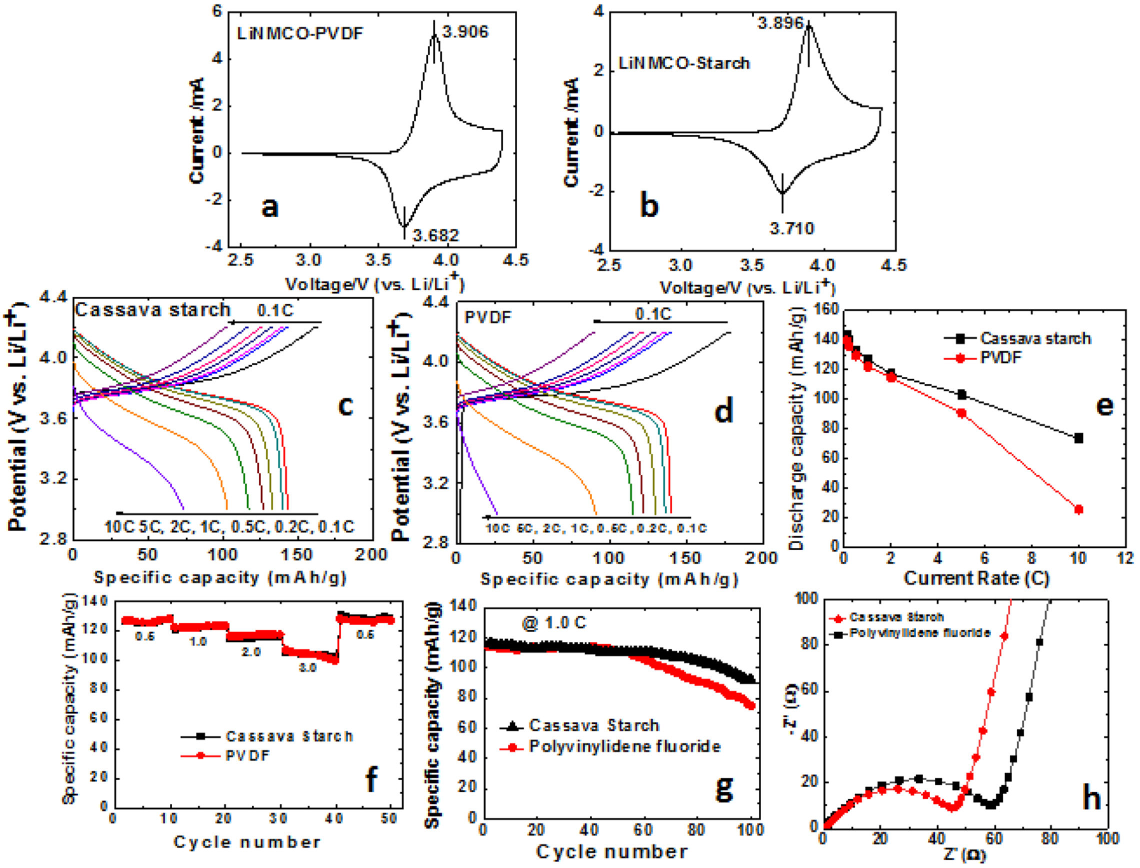

Fig. 3 Electrochemical properties of LiNMCO-442 cells with cassava starch and PVDF binders: **a, b** CV curves; **c, d** charge–discharge curves; **e** the current density as a function of discharge capacity; **f, g** galvanostatic rate and cycling performance; **h** EIS of LiNMCO-442 cells

Table 1 Redox peak potentials obtained from the CV data for the LiNMCO-442 electrode with the different binders

Electrode	Anodic peak (V)	Cathodic peak (V)	Peak separation (V)
LiNMCO-442 /PVDF	3.906	3.682	0.224
LiNMCO-442 /Cassava starch	3.896	3.710	0.186

In addition, charge/discharge curves of all the LiNMCO-442 cells depicted in Fig. 3c, d presented a similar charge/discharge plateau with a substantial amount of the charge storage capacity around 3.8–4.0 V. This behaviour matches the redox conversion of Ni^{2+}/Ni^{4+} in the backbone of LiNMCO-442. With an increasing charge/discharge rate of the LiNMCO-442 electrodes, there is an analogous decrease in the length of the plateau contributing to the charge storage capacity for both binders. As presented in Fig. 3c and d, the LiNMCO-442 cell with the cassava starch showed slightly higher discharged storage capacity from 0.1–1.0 C compared to the cells with PVDF, but a significant difference is observed at a higher C-rate (See Fig. 3e). This behaviour is due to the polarization of the LiNMCO-442 electrode at higher current density [27]. Furthermore, the improved charge–discharge profile may be attributed to the fact that cassava starch provided better networking and adhesion among the LiNMCO-442 particles and excellent contact between the electrode and the electrolyte. This is verified by the work of Masri et al. in Zn-air battery [19].

The cycle performance of the cells with the different polymeric binders is depicted in Fig. 3g. The LiNMCO-442 cells are compared at rate of 1.0C for 100 cycles, in the voltage range of 2.5–4.4 V. The LiNMCO-442 electrodes with the cassava starch binder revealed a higher initial discharge storage capacity of 116 mAh/g at a rate 1.0C compared to 113 mAh/g for PVDF cells. After 100 cycles, the LiNMCO-442 cells established discharge storage capacities of 91 and 74 mAh/g with retained discharge storage capacities of 80.2 and 65.5% for the cells with the cassava starch binder and the PVDF binder, respectively. Observing the performance of the cells comparatively, the cell with the cassava binder exhibited a steady voltage tendency, offering a fairly stable LiNMCO-442 electrode due to the strong binding effect of the aqueous starch binder. Cassava starch binder compared to the PVDF binder which is linear contains amylopectin units which are slightly branched chains, and this allows stress release when losing water during drying [28]. Furthermore, the existence of abundant hydroxyl functional groups in the starch chain assists binding with other functional groups attached to the LiNMCO-442 materials via hydrogen bonding and has proven to restore the structure of the electrode and provide strong adhesion and better mechanical properties [29, 30].

The resistance behaviour of the LiNMCO-442 electrode with the cassava starch was examined by EIS. The Nyquist plot displayed in Fig. 3h was measured within a frequency range of 10^{-2} to 10^{6} after the first charge/discharge cycle formation. The intercept on the real axis in the high-frequency region signifies the total resistance present in the electrolyte solution, including the electrode material, diffusion of the ions in the electrolyte, and the resistance between the active material and the current collector [31, 32]. The semi-circle is connected to the charge transfer resistance and the straight line in the low-frequency region is the lithium-ion diffusion in the LiNMCO-442 electrode with the cassava starch and PVDF binder. From the plot, it is found that the LiNMCO-442 with the cassava starch is characterized by a lower charge transfer resistance compared to the LiNMCO-442 with the PVDF binder. Lower charge transfer resistance demonstrates better Li^{+} and electron conductivity at the electro-active reaction sites. The improved rate capability and cycling performance of the LiNMCO-442 with the cassava starch may be a result of the improved electronic and ionic conductivity in the nickel-based electrode as demonstrated by Ismail et al. with the Zinc-air batteries electrodes employing cassava starch as a conductive binder [20].

Conclusions

The prepared electrode with the cassava starch binder showed fairly improved electrochemical performance over the commercially available petroleum-based binder, PVDF. The LiNMCO-442 electrodes prepared using the cassava starch showed better rate capability at a higher C-rate and superior cycle performance over the electrode with the PVDF binder. After 100 cycles, the LiNMCO-442 cells displayed discharge storage capacities of 91 and 74 mAh/g with retained storage capacities of 80.2 and 65.5% for the cells with cassava starch binder and PVDF binder, respectively, at a rate of 1C and a potential range of 2.5–4.4 V. From these preliminary results, the cassava starch stands the chance to be used in LIB, but further studies and modification would be needed to understand better its chemistry and electrochemical responses to enhance its performance.

Acknowledgments The research team would like to acknowledge the applied electrochemistry Laboratory at Hanbat National University, South Korea for supporting this work.

Data availability All data produced in this preliminary study have been included and discussed in this article. The data that support the findings of this study are available from the corresponding author upon reasonable request.

Declarations

Conflict of interest The authors declare no conflict of interest.

References

1. M. Alfred, H. Louis, L. Mohammed, K. Jang Myoun, Chem. Select 3(38), 10805–10810 (2018). https://doi.org/10.1002/slct.201802259
2. L. Mohammed, B. Chris Yeajoon, L. Kwang Se, H. Louis, K. Yong Il, L. Yun Jung, L. Yong Min, K. Jang Myoun, J. Electrochem. Sci. Technol. **9**(4), 330–338 (2018). https://doi.org/10.33961/JECST.2018.9.4.330
3. L. Mohammed, H. Mengyang, K. Sang Jun, B. Chris Yeajoon, K. Chiwon, C. Won Il, K. Jang Myoun, Solid State Ion. **319**, 7–12 (2018). https://doi.org/10.1016/j.ssi.2018.01.045
4. H. Louis, M. Alfred, L. Mohammed, L. Yong Min, K. Jang Myoun, B. Yeajoon Chris, K. Sang Jun, C. Won II, B. Yong Gu, P. Jong Woo, J. Ind, Eng. Chem. **53**, 241–246 (2017). https://doi.org/10.1016/j.jiec.2017.04.031
5. L. Mohammed, B. Bismark, M. Manasi, H. Louis, M. Alfred, N. Alex, M. Mutala, O. William, A. Francis Boateng, L. Yong Min, K. Jang Myoun, Korean J. Chem. Eng. **39**, 3003–3011 (2022). https://doi.org/10.1007/s11814-022-1210-4
6. K. Kwang Man, H. Lovely Rose, K. Jin-Chul, L. Young-Gi, K. Jang Myoun, Korean J. Chem. Eng. **32**(4), 717–722 (2015)
7. C. Hao, L. Min, H. Luke, L. Han Yeu, L. Gaoran, L. Zhan, L. Gao, Z. Shanqin, Chem. Rev. **118**(18), 8936–8982 (2018). https://doi.org/10.1021/acs.chemrev.8b00241
8. J.-T. Lin, Z.-Y. Wun, Y.-Q. Lum, Y. Zhou, Q.-S. Huang, L. Huang, S.-G. Sun, Adv. Energy Mater. **7**(24), 1701185 (2017). https://doi.org/10.1002/aenm.201701185
9. D. Bresser, D. Buchholz, A. Moretti, A. Varzi, S. Passerini, Energy Environ. Sci. **11**, 3096 (2018). https://doi.org/10.1039/c8ee00640
10. W. Ming, H. Jiazhi, W. Yikai, C. Yang-Tse, J. Electrochem. Soc. **166**(10), A2151–A2157 (2019). https://doi.org/10.1149/2.1171910jes
11. D.E. Malek, L.A. Malley, T.W. Slone, G.S. Elliott, G.L. Kennedy, W. Mellert, K. Deckardt, C. Gembardt, B. Hildebrand, S.R. Murphy, D.B. Bower, G.A. Wright, Drug Chem. Toxicol. **20**, 63–77 (1997). https://doi.org/10.3109/01480549709011079
12. S. Werner, S. Julian, H. Mathias Andreas, S. Stefan, Carbohydr. Polym. **265**, 118063 (2021). https://doi.org/10.1016/j.carbpol.2021.118063
13. N.C. Trupti, K.B. Bharat, V.J. Anjani, Int. J. Biol. Macromol **103**, 1032–1043 (2017). https://doi.org/10.1016/j.ijbiomac.2017.05.155
14. H. Vincent, J.K. Veronika, J. Stefan, E. Rolf, B. Alfred, F. Drita, L. Dominique, H. Philipp, Int. Arch. Occup. Environ. Health **87**(6), 663–674 (2014). https://doi.org/10.1007/s00420-013-0906-5
15. C.M. Fabrice, N. Svetlana, D. Dominique, A.-L. Yaser, D.J. Isobel, J. Power Sources **196**(4), 2128–2134 (2011). https://doi.org/10.1016/j.powsour.2010.10.025
16. S. Naresh, A. Shabbir, D.W. Dennis, J. Power Sources **378**, 660–670 (2018). https://doi.org/10.1016/j.jpowsour.2018.01.007
17. Z. Fang, L. Xiwei, P. Huawen, H. Xianluo, Z. Qiang Zhao, Adv. Funct. Mater. **30**(32), 2002169 (2020). https://doi.org/10.1002/adfm.202002169
18. K. Prasanna, T. Subburaj, Y.N. Jo, P. Santhoshkumar, S.K.S.S. Karthikeyan, K. Vediappan, R.M. Gnanamuthu, C.W. Lee, Sci Rep. **9**, 3318 (2019). https://doi.org/10.1038/s41598-019-39988-4
19. M.N. Masri, M.F.M. Nazeri, C.Y. Ng, A. Azmin Mohamad, J. King Saud Univ. Eng. Sci. (2013). https://doi.org/10.1016/j.jksues.2013.06.001
20. W.M.I.W. Ismail, M.N. Masri, H.K. Adli, IOP Conf. Ser.: Earth Environ. Sci. **596**, 012004 (2020). https://doi.org/10.1088/1755-1315/596/1/012004
21. G.A. Richard, K. Bhanu, Science **297**, 803–807 (2002). https://doi.org/10.1126/science.297.5582.803
22. I. Dueramae, M. Okhawilai, P. Kasemsiri, H. Uyama, R. Kita, Sci Rep **10**, 12587 (2020). https://doi.org/10.1038/s41598-020-69521-x
23. S. Enomoto, Y. Kawai, M. Sugita, J Polym Sci A–2 **6**, 861 (1968). https://doi.org/10.1002/pol.1968.160060506
24. M. Ling, Y.N. Xu, H. Zhao, X.X. Gu, J.X. Qiu, S. Li, M.Y. Wu, X.Y. Song, C. Yan, G. Liu, S.Q. Zhang, Nano Energy **12**, 178–185 (2015). https://doi.org/10.1016/j.nanoen.2014.12.011
25. J. Liu, Q. Zhang, T. Zhang, J.-T. Li, L. Huang, S.-G. Sun, Adv Funct Mater **25**, 3599–3605 (2015). https://doi.org/10.1002/adfm.201500589
26. X. Jing, L. Feng, D.M. Marc, T. Wei, J. Mater. Chem. A **5**, 874–901 (2017). https://doi.org/10.1039/C6TA07991A
27. X. Jiantie, C. Shu-Lei, G. Qin-fen, L. Hua-Kun, D. Shi-Xue, J. Power Sources **225**, 172–178 (2013). https://doi.org/10.1016/j.jpowsour.2012.10.033
28. M.M.J. Bianca, G.J.J. Walter, B.M.A.M. Erik, S.A. Henk, J. Anim. Sci. Biotechnol. **9**, 91 (2018). https://doi.org/10.1186/s40104-018-0303-8
29. B. Dominic, B. Daniel, M. Arianna, V. Alberto, P. Stefano, Energy Environ. Sci. **11**, 3096–3127 (2018). https://doi.org/10.1039/C8EE00640G
30. T. Zhang, J. Li, J. Liu, Y. Deng, Z. Wu, Z. Yin, D. Guo, L. Huang, S. Sun, Chem. Commun. **52**(25), 4683–4686 (2016). https://doi.org/10.1039/c5cc10534j
31. Y. Chen, M.L. Zhang, Z.H. Shi, J. Electrochem. Soc. **152**, A1272–A1278 (2005). https://doi.org/10.1149/1.1904912
32. J. Gamby, P.L. Taberna, P. Simon, J.F. Fauvarque, M. Chesneau, J. Power Sources **101**, 109–116 (2001). https://doi.org/10.1016/S0378-7753(01)00707-8